

CARRIER TRANSPORT MECHANISMS IN ION-IMPLANTED SILICON-ON-INSULATOR STRUCTURES WITH InSb CLUSTERS

Alexander K. Fedotov¹⁾, Ida Tyschenko²⁾, Julia Fedotova¹⁾, Alexey Pashkewich^{1), 3)}, Ivan Svito³⁾

¹⁾*Institute for Nuclear Problems, Belarusian State University,
11 Babrujskaja Str., 220030 Minsk, Belarus*

²⁾*A.V. Rzhanov Institute of Semiconductor Physics,
13 Lavrentyev Avenue, 630090 Novosibirsk, Russia*

³⁾*Belarusian State University, 4 Nezavisimosti Ave., 220030 Minsk, Belarus*

In this paper, we examine carrier transport mechanisms in Silicon-on-Insulator (SOI) structures, containing InSb nanoparticles in SiO₂ layer, before and after annealing at 1273 K. The comparison of temperature dependences of current-voltage (I-V) characteristics allowed us to determine the mechanisms of carrier transport (hopping and zone-like) in this nanostructures and estimate some transport parameters in the temperature range of 2-300 K. The measurements have confirmed the presence of Foulmer-Nordheim and hopping mechanism contributions into low-temperature I-V characteristics of the studied SOI structures.

Keywords: SOI structures; InSb nanoparticles; Silicon oxide; I-V characteristics; carrier transport.

Introduction

To produce different functional elements on the overall silicon platform with the increased integral circuits (IC) operation rate, many of hybrid structures are developed. Among them, the nano dimensional A₃B₅ compound crystals combined with a well established Si-based technology are proposed to attain these objectives [1-6]. Among all A₃B₅ compounds, direct energy band structure of InSb and high values of electron and hole mobilities (80,000 and 1250 cm²/V·s, respectively) provides its suitability to the increasing IC operation rate [3] and high quantum efficiency that allows the applicability of this compound in optoelectronics. These nanocrystals are ideal objects for detecting a quantum-size effects due to very small values of the effective masses of charge carriers (0.015m₀ for electrons and 0.39m₀ for holes) as well as spin-orbital splitting [7-9].

The silicon dioxide dielectric constant modification by the incorporation of InSn nanocrystals (NPs) is very important for the design of memory devices, as well as for modeling the gate dielectric characteristics [10-12]. These NPs incorporated into a dielectric matrix should exhibit specific current-voltage (I-V) characteristics as well due to particular tunneling mechanisms of

charge carrier transport between NPs [14, 15].

InSb nanocrystals, embedded into SiO₂ layers, being important materials for modern electronics and optoelectronics, can be formed using ion-beam techniques [4,5]. An additional influencing technological factor for manufacturing of such devices is post-implantation annealing as well, which causes changes both in crystalline and band structure of the formed phases [6].

Therefore, InSb can be considered as an alternative materials when creating hybrid thin-film silicon-based structures. However, compared to other semiconductor materials, there is not so much literature data on the carrier transport in InSb-NPs/SiO₂ based thin-film nanostructures. So, the purpose of this paper to present the results of carrier transport mechanisms depending on temperature and structural peculiarities of the modified SiO₂ layers with buried InSb NPs in Silicon-on-Insulator (SOI) nanostructures which are responsible for their striking electronic properties.

Experimental

In this paper we study carrier transport properties in SOI structures containing InSb NPs in the buried SiO₂ layer were produced by the DeleCut technology described in [16].

They were manufactured using 300 nm thick silica layer, which was grown by heating a p-type (100) silicon wafer with 100 mm diameter, in which In^+ and Sb^+ ions were implanted with energies of 200 keV in doses of $8 \times 10^{15} \text{ cm}^{-2}$ (Fig. 1). We have studied both initial (pristine) samples after implantation and samples subjected to post-implantation annealing in an atmosphere of N_2 at the temperatures $T_a = 1273 \text{ K}$ for 30 minutes. Details of manufacturing and annealing procedures as well as the structural properties of SOI samples are presented in [5, 6].

The current-voltage (I-V) characteristics of the modified SiO_2 layers were measured on samples $2 \times 3 \text{ mm}^2$ in size as a function of the temperature that was ranged from 30 K to 300 K using a close-cycle Cryogen-Free Measuring System (CFMS, Cryogenic Ltd., London). For this purpose, the 50 mm thick Al foils were spark welded on rear and front sides of the as-implanted and annealed samples. Then, indium contacts with copper wires 0.1 mm in diameter were attached to aluminum by ultrasonic soldering. Then these wires were soldered to the gold-plated electrical contacts of a special measuring cell. The cell with the sample was inserted into a special measuring probe, which was placed in a cryostat and connected to the measuring circuit. The measurement details were described in [13].

Results and discussion

Examples of the experimentally measured temperature dependences of the transversal I-V characteristics in the implanted and annealed samples are shown in Fig. 1. As can be seen, the I – V characteristics of both samples are asymmetric and after annealing have no hysteresis practically. In addition, at the same applied bias voltages U , slightly less currents flow through the initial (unannealed) sample than those of the annealed one, which indicates more low-Ohmic behaviour of the latter. This fact can be associated with the shunting effect of InSb nanoparticles inside the dielectric layer of SiO_2 (since the resistance of InSb is obviously lower than

that of silicon oxide, including due to disordering of silicon oxide by implantation.

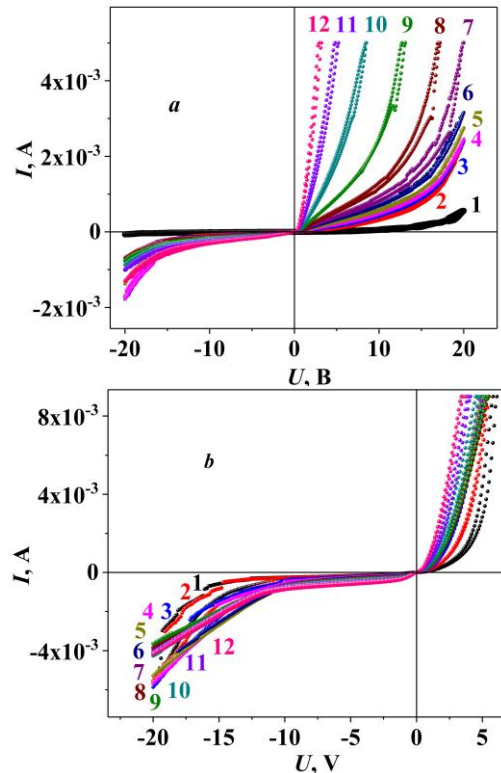


Fig. 1. I-V characteristics of the pristine (a) and annealed (b) samples at different temperatures T , K: 1 - 30; 2 - 50; 3 - 75; 4 - 100; 5 - 125; 6 - 150; 7 - 175; 8 - 200; 9 - 225; 10 - 250; 11 - 275; 12 - 300

To reveal the mechanisms of carrier transport in the studied samples, the experimental I-V characteristics in the form of dependences of current I (current density J) on bias voltage U (electric field strength E) and temperature T were rearranged in coordinates corresponding to different models of carrier transport for metal-insulator-semiconductor structures, which would give linearization in any range of temperatures and (or) electric field strengths.

As can be seen from Fig. 1a, for an unannealed sample in weak electric fields, the experimental I-V characteristics are well linearized in Arrhenius coordinates $\log I(U = \text{const}) - (1/T)$ at low temperatures, while for the annealed sample in Fig. 1b, such linearization of the curves is not observed.

At the same time, as follows from Fig. 2, linearization in the coordinates $\log (J/E^2) - (1/E)$ takes place in strong electric fields.

In accordance with the Fowler-Northheim

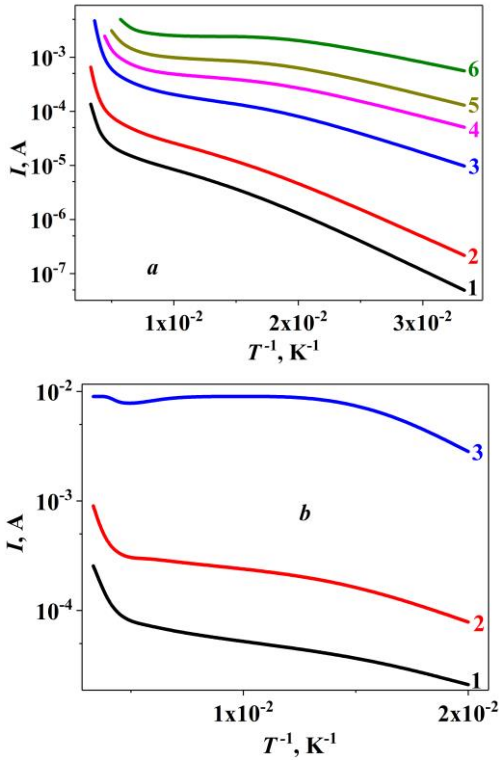


Fig. 2. Temperature dependences of the I–V characteristics of the pristine (a) and annealed (b) samples at different bias voltages U , V: 1 - 0.5; 2 - 1.0; 3 - 5.0; 4 - 10.0, 5 - 15.0; 6 - 20.0

this case, as can be seen from the comparison of Fig. 2a and 2b, the current density in which this linearization manifests itself in the annealed sample strongly depends on temperature, in contrast to the initial (unannealed) ones.

model [17], if the strong field criterion is satisfied, $eE > \varphi_0$, that is, at $(5-7) \cdot 10^6$ B/cm, the described behavior of the I–V characteristic corresponds to tunneling of charge carriers between InSb nanoparticles and is described by the relation

$$J(V, T) = 1.54 \times 10^{-6} \frac{E^2}{\varphi_0} \exp\left(-6.7 \times 10^6 \frac{\alpha^* \varphi_0^3}{E}\right) \quad (1)$$

This behavior means that, after annealing, the tunneling current in the investigated temperature range is significantly higher than that of an unannealed sample. Within the framework of this model (1), it is possible to determine the activation energy (in fact, the barrier height φ_0) corresponding to the I–V characteristic curves in Fig. 2. The estimates have shown that the barrier height of the initial

SOI structure (before annealing) is significantly higher than in the annealed sample, however, in both cases, it slightly decreases with increasing temperature in the region of $30 < T < 300$ K: from 154 meV to 131 meV after implantation and from 106 meV to 99 meV for the sample after annealing.

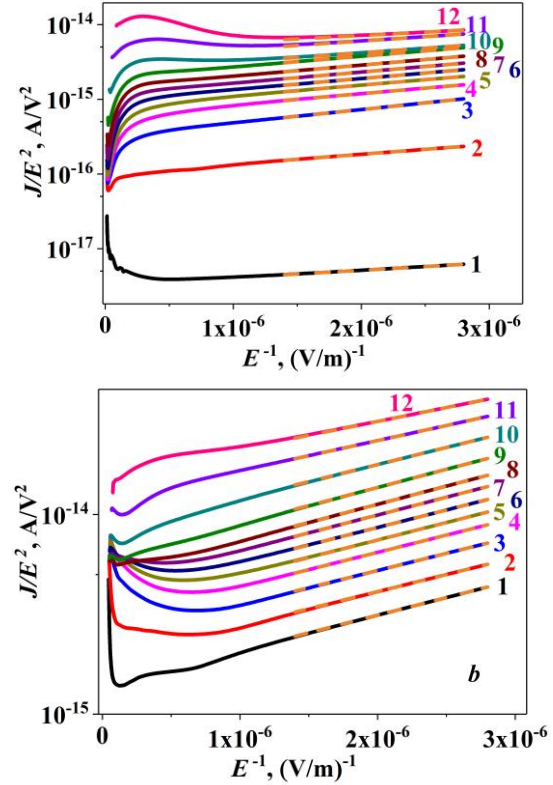


Fig. 3. Electric field dependences of the I–V characteristics of the initial (a) and annealed (b) samples at different temperatures T , K: 1 - 30; 2 - 50; 3 - 75; 4 - 100; 5 - 125; 6 - 150; 7 - 175; 8 - 200; 9 - 225; 10-250; 11 - 275; 12 - 300

The estimates made allow us to explain the important feature of the described above behavior of I–V characteristics: after the formation of InSb nanoparticles in the buried SiO₂ layer due to annealing of SOI structures I–V characteristics becomes to be changed significantly weaker with temperature. This can be explained by two reasons. The first of them consists in the aforementioned shunting effect of InSb nanoparticles, which form a second (parallel) channel of electrical transfer in the dielectric matrix due to the smaller, than that of silicon oxide, the band gap of indium antimonide. The second reason is due to the strong disordering of the implanted

silicon oxide layer prior to annealing.

On the whole, as can be seen from the figures presented and follows from the estimates made, the difference in the I–V characteristics of annealed and un-annealed samples is manifested mainly in weak electric fields (when the Fowler-Northheim model is not working). In strong fields, the I–V characteristics are determined, first of all, by the structural state of the silicon oxide layer, and the presence of InSb particles plays a lesser role. It can also be expected that, in the samples of un-annealed SOI structures, a certain role in the formation of the I–V characteristic can play the hopping of electrons by the localized states that have arisen as a result of implantation. However, this issue requires additional research.

Resume

Based on the study of the temperature dependences of I-Vs in un-annealed and annealed at 1273 K SOI structures, it shows that in the temperature range of 30 - 300 K in strong electric fields, electric transport is realized by the Fowler-Nordheim tunneling mechanism. The estimates of the barrier heights ϕ_b , conducted within the framework of the model (1) in the temperature range of 30 - 300 K, gives the values $130 < \phi_b < 150$ meV for the initial and $99 < \phi_b < 110$ meV for the annealed samples.

References

1. Ko H., Takei K., Kapadia R., Chuang S., Fang H., Leu P.W. et al. Ultrathin compound semiconductor on insulator layers for high-performance nanoscale transistors, *Nature* 2010; 468: 286-289.
2. Ford A.C., Yeung C.W., Chuang S., Kim H.S., Plis E., Krishna S. et al. Ultrathin body InAs tunneling field-effect transistors on Si substrates, *Appl. Phys. Lett.* 2011; 98: 113105-1-6.
3. Takei K., Kapadia R., Fang H., Plis E., Krishna S., Javey A. High quality interfaces of InAs-on-insulator field-effect transistors with ZrO₂ gate dielectrics, *Appl. Phys. Lett.* 2013; 102: 153513.
4. Prucnal S., Zhou Sh, Ou X., Facsko S., Liedke M.O., Bregolin F. et al. III-V/Si on silicon-on-insulator platform for hybrid nanoelectronics, *J. Appl. Phys.* 2014; 115: 074306.
5. Zukowski P., Koltunowicz T., Czarnacka K., Fedotov A.K., Tyschenko I.E. Charge carrier transport and dielectric permittivity in SiO₂ films with InSb nanoparticles. International Forum “Microelectronics – 2020”. XIII International conference «Silicon – 2020». Abstract book: Crimea Republic, Yalta September 21–25, 2020 / Ed. by E.S. Gornev. Moscow: MAKS Press, 2020. p. 112-114. (In Russian).
6. Zukowski P., Koltunowicz T.N., Czarnacka K., Fedotov A.K., Tyschenko I.E. Carrier transport and dielectric permittivity of SiO₂ films containing ion-beam synthesized InSb nanocrystals. *J. Alloys Compd.* 2020; 846-861.
7. Igarashi Y., Jung M., Yamamoto M., Oiwa A., Machida T., Hirakawa K., Tarucha S. Spin-half Kondo effect in a single self-assembled InAs quantum dot with and without an applied magnetic field, *Phys. Rev. B* 2007; 76: 081303(R).
8. Takahashi S., Igarashi Y., Deacon R.S., Oiwa A., Shibata K., Hirakawa K., Tarucha S. Quantitative evaluation of spin-orbit interaction in InAs quantum dots, *J. Phys.: Conf. Ser.* 2009; 150: 22084-1-5.
9. Zhang X.W., Xia J.B., Rashba spin-orbit coupling in InSb nanowires under transverse electric field, *Phys. Rev. B* 74 (2006): 075304-1-4.
10. Tiwari S., Rana F., Hanafi H., Hartstein A., Crabbe E.F., Chan K. A silicon nanocrystals based memory, *Appl. Phys. Lett.* 1996; 68: 1377-1379.
11. Lombardo S., De Salvo B., Gerardi C., Baron T. Silicon nanocrystal memories, *Microelectron. Eng.* 2004; 72: 388-394.
12. Dimitrakis P., Kapetanakis E., Tsoukalas D., Skarlatos D., Bonafos C., Ben Assayag G. et al. Silicon nanocrystal memory devices obtained by ultra-low-energy ion-beam synthesis, *Solid State Electron.* 2004; (48): 1511-1517.
13. Fedotov A.K., Prischepa S.L., Fedotova J.A., Bayev V.G., Ronassi A.A., Komissarov I.V. et al. Electrical conductivity and magnetoresistance in twisted graphene electrochemically decorated with Co particles, *Physica E: Low-dimensional Systems* 2020; 117: 113790-1-5.
14. Koltunowicz T.N., Zukowski P., Czarnacka K., Bondariev, Boiko O., Svito I.A., Fedotov A.K. Dielectric properties of nanocomposite (Cu)_x(SiO₂)_(100-x) produced by ion-beam sputtering, *J. Alloys Compd.* 2015; 652: 444-449.
15. Zukowski P., Koltunowicz T.N., Bondariev V., Fedotov A.K., Fedotova J.A. Determining the percolation threshold for (FeCoZr)_x(CaF₂)_{100-x} nanocomposites produced by pure argon ion-beam sputtering, *J. Alloys Compd.* 2016; 683: 62-66.
16. Tyschenko I.E., Voelskow M., Cherkov A.G., Popov V.P. Ion-beam synthesis of InSb nanocrystals in the buried SiO₂ layer of a silicon-on-insulator structure. *Semiconductors* 2014; 48: 1196-1201.
17. Chen D., Li C., Zhu Z., Fan J., Wei S. Interface effect of InSb quantum dots embedded in SiO₂ matrix. *Phys. Rev. B* 2005; 72(7): 075341-1-7.